Tailoring the Local Environment of Quantum Dots for Enhanced Collection Efficiency

F. Hakan Köklü[1], A. N. Vamivakas[2], B. B Goldberg[1], and M. S. Ünlü[1]
[1]Department of Electrical and Computer Engineering, Boston University, 8 Saint Mary's Street, Boston
[2]Cavendish Laboratory, University of Cambridge, JJ thompson Avenue, Cambridge, UK

***Abstract*— We theoretically demonstrate that location of a dipole emitter with respect to the interface significantly affects the collected signal intensity. Optimally engineered samples can provide 4 fold enhancement in collection.**

I. Introduction

Wide use of high numerical aperture (NA) objectives in fluorescence microscopy and quantum dot spectroscopy triggered a research effort to model the dipole emission, collection and imaging [1], [2] using the angular spectrum representation [3], [4] (ASR). Further studies focused on the collection of dipole emission near an interface [5]. Increasing the light interaction with quantum dots represents an important aspect for quantum information science [6]. In this work, we study the collection of light emitted from a dipole embedded in a high refractive index medium near an interface. Our computations simulate the collection of light emitted from a quantum dot located in GaAs for near an air and metal interfaces using ASR. We show that for each case, the reflection of emission from the interface causes interference resulting in significant enhancement of collection - up to 4 fold for metal interface - for optimally engineered structures.

II. Theory

The optical system illustrated in Fig. 1 is aplanatic. Reference sphere 1 is referred as collection objective and reference sphere 2 as focusing objective. We assume the dipole $\mathbf{d}$ is placed at the focus of the collection objective. We define the relevant angles, unit vectors, and wave vectors in Fig. 1. Fig. 2(a) shows a more real-like setup configuration. The dipole is located close to the far interface and imaged using a central solid immersion lens [7], [8]. Central solid immersion lens allows us to ignore the interface close to the objective thus making $n_1 = 3.5$ as in GaAs..

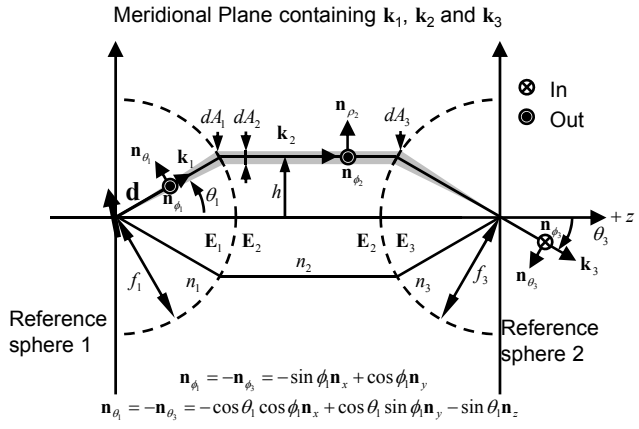

Fig. 1. Optical system geometry used to image an arbitrarily oriented dipole.

The first step will be writing the dipole field, $\mathbf{E}_1$, at the first lens (focal length = f_1) in a way that will ease manipulation later.

$$\mathbf{E}_1 = \frac{\omega^2}{\epsilon_0 c^2}\frac{e^{ik_1 f_1}}{4\pi f_1}\widetilde{\mathbf{G}}_T\mu = \frac{\omega^2}{\epsilon_0 c^2}\frac{e^{ik_1 f_1}}{4\pi f_1}\mathbf{E}_d \tag{1}$$

where $\widetilde{\mathbf{G}}_T = \widetilde{\mathbf{G}}_0 + \widetilde{\mathbf{G}}_r$, Green's functions for original and reflected field [3]. To calculate the image of the dipole, we employ ASR and express the image dipole field as

$$\begin{aligned} E_3 \quad &= \frac{\omega^2}{\epsilon_0 c^2}\frac{e^{ik_1 f_1}}{4\pi f_1}\frac{ik_3 f_3 e^{-ik_3 f_3}}{2\pi} \\ &\int_0^{\theta_{max3}}\int_0^{2\pi}[-(\mathbf{E}_d\cdot\hat{\mathbf{n}}_{\phi_1})\hat{\mathbf{n}}_{\phi_3} - (\mathbf{E}_d\cdot\hat{\mathbf{n}}_{\theta_1})\hat{\mathbf{n}}_{\theta_3}] \\ &e^{ik_3 z cos\theta_3}e^{ik_3\rho sin\theta_3 cos(\phi_3-\varphi)}sin\theta_3\sqrt{\frac{cos\theta_3 n_1}{cos\theta_1 n_3}}d\phi_3 d\theta_3 \end{aligned} \tag{2}$$

After necessary transformations and simplifications, the end result is as follows;

$$\begin{aligned} &\mathbf{E}_3 = C_0 C_1 \pi \\ &\left\{\mu_x\begin{bmatrix} I_0 + I_2 cos2\varphi \\ I_2 sin2\varphi \\ -2iI_{1m}cos\varphi \end{bmatrix} + \mu_y\begin{bmatrix} I_2 sin2\varphi \\ I_0 - I_2 cos2\varphi \\ -2iI_{1m}sin\varphi \end{bmatrix} + \right. \\ &\mu_z\begin{bmatrix} 2iI_1 cos\varphi \\ 2iI_1 sin\varphi \\ -2I_{0m} \end{bmatrix} + \mu_x\begin{bmatrix} I_0^r + I_2^r cos2\varphi \\ I_2^r sin2\varphi \\ 2iI_{1m}^r cos\varphi \end{bmatrix} + \\ &\left.\mu_y\begin{bmatrix} I_2^r sin2\varphi \\ I_0^r - I_2^r cos2\varphi \\ 2iI_{1m}^r sin\varphi \end{bmatrix} + \mu_z\begin{bmatrix} 2iI_1^r cos\varphi \\ 2iI_1^r sin\varphi \\ -2I_{0m}^r \end{bmatrix}\right\}\begin{bmatrix} n_x \\ n_y \\ n_z \end{bmatrix} \end{aligned} \tag{3}$$

where,

$$I_0 = \int_0^{\theta_{max3}}(1 + cos\theta_1 cos\theta_3)sin\theta_3 J_0(k_3\rho sin\theta_3)d\theta_3 \tag{4}$$

and $g(\theta) = \sqrt{\frac{cos\theta_3 n_1}{cos\theta_1 n_3}}e^{ik_3 z cos\theta_3}e^{-ik_1 cos\theta_1 z_0}$, $C_0 = \frac{\omega^2}{\epsilon_0 c^2}\frac{e^{ik_1 f_1}}{4\pi f_1}$, $C_1 = \frac{ik_3 f_3 e^{-ik_3 f_3}}{2\pi}$ and r_s, r_p are the Fresnel reflection coefficients. The rest of the integrals are not shown due to space limitations.

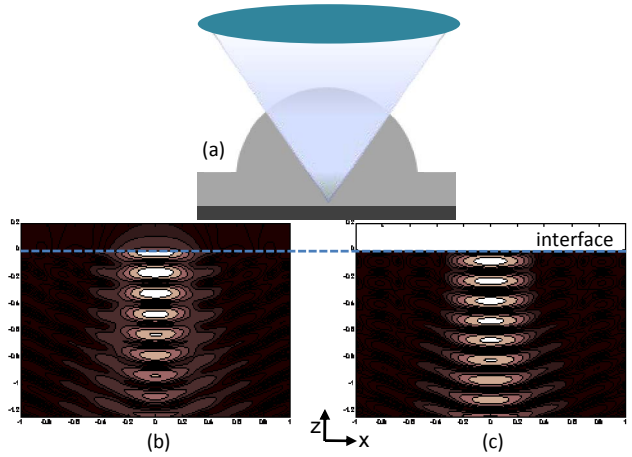

Fig. 2. (a) Focusing and collection geometry. (b) Excitation focal field distribution near a GaAs-air interface. (c) Same as (b) but for a GaAs-metal interface. x-axis range is [-λ_0 λ_0] and z-axis range is [$-1.2\lambda_0$ $0.2\lambda_0$]. Dashed line corresponds to the location of the interface.

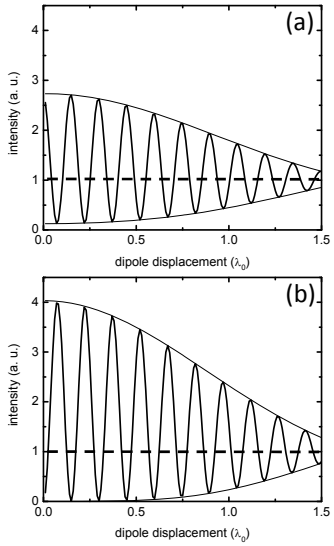

Fig. 3. (a) Imaged maximum intensities for a dipole located near a GaAs-air interface. (b) Same as (a) but for a GaAs-metal interface. Dashed line corresponds to the case when there is no interface.

III. Results

Since we assumed that the dipole is placed at the focus of the collection objective, defocus parameter, z_0, is nonzero for only the reflected field. This means every different simulation is valid for a different sample with a dipole located at a different depth. We conducted the calculations for a horizontally aligned dipole which is usually the case for quantum dots. Our collection objective has a fairly low numerical aperture (NA) of 0.4 since solid immersion imaging necessitates the use of high working distance objectives. However, our conclusions will be also valid for high NA objectives where solid immersion microscopy will be difficult to conduct. The collection NA in the case of solid immersion lens is $nsin\theta = 0.4 \cdot 3.5 = 1.4$ comparable to conventional high NA optics. Focusing objective's NA is 0.14. Before calculating the dipole emission, understanding the excitation focal field distribution will be helpful to interpret our results. As seen in Fig. 2(b), for both interfaces there are hot spots due to the interference of excitation light with its reflection. The depicted distributions are valid for focusing in $\sim \lambda_0/2$ vicinity of the interface. Following this, we examined the dipole emission when the dipole is displaced in range of from 0 to $1.5\lambda_0$ from the interface where λ_0=950nm. Fig. 3 shows the results for a GaAs-air and GaAs-metal interface. The plots display the maximum intensities normalized with respect to no-interface case and calculated for different dipole locations. The dashed line corresponds to the no-interface case. As seen in Fig. 3, collected light can be enhanced nearly 3 fold for a GaAs-air interface and 4 fold for a GaAs-metal interface, respectively, for optimally engineered samples. The maximums are located at $\lambda_0/2n_1$ and $\lambda_0/4n_1$, respectively, for air and metal interfaces. The period for each case is $\lambda_0/2n_1$. In addition, these spots coincide with the excitation hot spots. On the other hand, poorly designed samples can result in almost no collection due to poor excitation and collection efficiency. The envelope functions in Fig. 3 correspond to the cases of full constructive and destructive interference between the original field and reflected field.

IV. Conclusions

We computed the collection of dipole emission near a dielectric and metal interface using the full vector field approach of ASR. Our calculations show that for a quantum dot sample without any coating on it, reflected field from the air interface can increase the collection efficiency nearly a factor of 3. For a modified sample with a metal interface, this increase can be as much as a factor of 4. The excitation field distribution also follows the same pattern, making potential measurements easier. However, improperly designed samples may produce almost zero excitation and collection. We are currently working on experimental validation of these results.

References

[1] J. Enderlein, "Theoretical study of detection of a dipole emitter through an objective with high numerical aperture," *Opt. Lett.*, vol. 25, p. 634, May 2000.

[2] A. N. Vamivakas, S. B. Ippolito, M. Dogan, B. E. R., A. K. Swan, B. B. Goldberg, and M. S. Ünlü, "Phase-sensitive detection of dipole radiation in a fiber-based high numerical aperture optical system," *Opt. Lett.*, vol. 32, p. 970, April 2007.

[3] L. Novotny and B. Hecht, *Principles of Nano-Optics*. Cambridge University Press, 2006.

[4] B. Richards and E. Wolf, "Electromagnetic diffraction in optical systems. ii. structure of the image field in an aplanatic system," *Proc. R. Soc. London A*, vol. 253, p. 358, December 1959.

[5] J. Enderlein and M. Bohmer, "Influence of interface-dipole interactions on the efficiency of fluorescence light collection near surfaces," *Opt. Lett.*, vol. 28, p. 941, June 2003.

[6] A. N. Vamivakas, M. Atatüre, S. T. Dreiser, J. Yilmaz, A. Badolato, A. K. Swan, B. B. Goldberg, A. Imamoglu, and M. S. Ünlü, "Strong extinction of a far-field laser beam by a single quantum dot," *Nano Lett.*, vol. 7, no. 9, p. 2892, 2007.

[7] S. B. Ippolito, B. B. Goldberg, and M. S. Ünlü, "Theoretical analysis of numerical aperture increasing lens microscopy," *J. Appl. Phys.*, vol. 97, p. 053105, 2005.

[8] Z. Liu, B. B. Goldberg, S. B. Ippolito, A. N. Vamivakas, M. S. Ünlü, and R. Mirin, "High resolution, high collection efficiency in numerical aperture increasing lens microscopy of individual quantum dots," *Appl. Phys. Lett.*, vol. 87, p. 071905, 2005.